

# Evaluation of the Metal Artifact Caused by Dental Implants in Cone Beam Computed Tomography Images

Nazmehr VAHDANI<sup>a</sup>, Ehsan MOUDI<sup>b</sup>, Fatemeh GHOBADI<sup>a</sup>, Ebrahim MOHAMMADI<sup>a</sup>, Ali BIJANI<sup>c</sup>, Sina HAGHANIFAR<sup>b</sup>

<sup>a</sup>Oral and Maxillofacial Radiology, Student Research Committee,

Babol University of Medical Sciences, Babol, Iran

<sup>b</sup>Oral Health Research Center, Health Research Institute,

Babol University of Medical Sciences, Babol, Iran

<sup>c</sup>Social Determinants of Health Research Center, Health Research Institute,

Babol University of Medical Sciences, Babol, Iran

## ABSTRACT

**Statement of the problem:** The presence of a metal object such as dental implants in the scan field may cause artifacts on the cone-beam computed tomography (CBCT) images, which can reduce the diagnostic quality and accuracy of images.

**Purpose:** The aim of this in vitro study was to compare the severity of implant-induced metal artifacts on CBCT images.

**Materials and method:** To this end, a dry human mandible and a maxilla were selected, then two Roxolid and two Zirconium fixtures with different diameters were placed in the central incisor and first molar sockets and fixed with dental wax. The mandible and maxilla were placed in the simulated phantom for soft tissue, and the occlusal plane was adjusted parallel to the horizon. Images were taken at standard and high resolutions using two CBCT units. The CBCT gray values were measured in three longitudinal sections of the fixture (cervical, middle and apical) and the contrast noise ratio (CNR) was calculated. The CNR values of images were analyzed based on the fixture material, resolution, jaw, unit parameters and fixture size by using the paired t-test and different fixture sections by one-way ANOVA.

**Results:** Depending on the CBCT unit, the CNR values in Roxolid and Zirconium fixtures are completely different. Under higher exposure parameters, the CNR values of the Roxolid and Zirconium fixtures were

Address for correspondence:

Sina Haghanifar, Professor

School of Dentistry, Babol University of Medical Sciences, Ganj Afrooz Ave, Babol, Iran

Tel./Fax: +98-11-322-91408

Article received on the 12<sup>th</sup> of December 2019 and accepted for publication on the 1<sup>st</sup> of June 2020

significantly higher in the maxilla than mandible. However, the fixture size and longitudinal section type did not have a significant effect on the CNR values.

**Conclusion:** In contrast to the fixture material, scanning parameters and jaw type, differences in the size and longitudinal section of the fixtures had no impact on artifact severity.

**Keywords:** dental implants, artifact, cone-beam computed tomography.

## INTRODUCTION

Dental implants are a suitable choice for edentulous regions in the jaw with high success rate and desired outcomes. The application of CBCT in the treatment plan increases the chance of long-term dental implant success (1). CBCT is also used in other dental branches for the diagnosis, treatment plan, and follow-up (2-4).

As compared to CT, the lower cost, fast acquisition, and lower radiation dose have made CBCT increasingly popular in dentistry. The CBCT advantages include high accuracy and high resolution, and removal of burning and overlap of adjacent teeth (5, 6). The presence of a metal object in the scan field may cause artifacts in CBCT images which, in turn, reduces image quality and sometimes makes it unclear (6). The presence of a fixture in the CBCT scan field weakens the x-ray beam, inhibiting the proper scan of structures adjacent to the implant site (7). The conical nature of the X-ray beam causes artifacts in all areas around the implant site (6, 8). The artifact severity depends on the shape, position, direction, and number of implants in the image, and also on the sequence of related parameters. Many variables are involved with the incidence of artifacts, such as exposure conditions, pixel size, and field of view (FOV) (9-10).

There are some studies into the use of artifact reduction algorithm (11, 12). Although these algorithms can partially reduce the incidence of artifacts, the details around the metal-tissue interface, as the main region of interest (ROI), may still remain unobservable to the clinicians (13). Therefore, the effects of factors capable of reducing metal-related artifacts in CBCT imaging should be assessed.

The most common artifacts are black or white strip and streak lines, as well as dark area around a hard and metal object depending on the extent

to which the ray is weakened or absorbed by a high-density substance (14-16).

This study was conducted to determine the severity of implant-related artifacts in different maxillary and mandibular areas based on the size, site, and implant material, using the CBCT units set at standard and high resolutions. □

## MATERIALS AND METHOD

After ethical approval was given by Babol University of Medical Sciences (IR.MUBABOL.HRI.REC.1397.187), this study used intact dry human mandible and maxilla with empty sockets at central incisor and first molar sites.

Four Straumann fixtures (ITI, Basel, Switzerland)

Including two Zirconium fixtures:

(PURE Ceramic, Monotype, Cylindrical: 4.1×10 mm)

(PURE Ceramic, Monotype, Cylindrical: 3.3×10 mm)

And two Roxolid fixtures:

(Roxolid\*, Standard Plus, Cylindrical: 4.1×10 mm)

(Roxolid\*, Standard Plus, Cylindrical: 3.3×10 mm)

\*Roxolid: 85% Titanium and 15% Zirconium

Two plastic cylinders with the least severity of artifact were used to fix the jaws during the scan. In addition, water was used for simulating the soft tissue (17).

Scans were taken using two CBCT units X MIND (ACTEON, Olgiate Olona, Italy) and 5G (Newtom, Verona, Italy) at two different resolutions (high, standard) in the presence and absence of fixtures (as the case and control groups, respectively). The X MIND scan parameters were set as follows: 90 kVp, current of 8 mA, FOV of 11×8 cm and pixel size of 150 μ at standard resolution and 100 μ at high resolution.

The 5G scan parameters were set as follows: 110 kVp, current of 10 mA, FOV of 12×8 cm

and the pixel size of 150 μ at standard resolution and 75 μ at high resolution.

The XMIND images were analyzed with OnDemand 3D Dental, and 5G images were analyzed with NNT software. First, the mandible with empty sockets in the central incisor and first molar sites was placed in the plastic phantom filled with water (if needed, thermal adhesive was used at the condyles to attach it to the cylinder and position the occlusal plane parallel to the horizon). Then, CBCT images were taken at standard and high resolution, using XMIND and 5G units (control group). Next, the Roxolid fixture (diameter 3.3 mm) was placed in the central incisor socket, that the total 10 mm height of the fixture was in the bone (crestal) and fixed upright by wax. The same procedures were applied to the central incisor socket using the Zirconium fixture (diameter 3.3 mm). Then, the anterior fixture was removed from the socket and the Roxolid fixture (diameter 4.1 mm) was placed in the first molar socket and scanned using the same units at standard and high resolutions. The same procedures were conducted with the Zirconium fixture (diameter 4.1 mm). In total, 40 CBCT scans were performed (32 scans in the case group and eight scans in the control).

To standardize ROI positions and include the artifact areas, the 10 mm fixture heights in the images were divided into the cervical, middle, and apical sections (2 mm, 5 mm, and 8 mm, respectively). In the axial view of each section, a line was drawn from the fixture center along the longitudinal axis of the jaw, then, a perpendicular line and three lines spaced 25° from each other was drawn (two anterior lines at angles of 115° and 140°, and one anterior line at an angle of 65°). To examine the fixtures at the anterior area, only the lines at the angles of 65°, 90°, and 115° were drawn. Moreover, three semicircles (1.5 cm, 2 cm and 2.5 cm in diameter) were drawn from the fixture center, resulting in a total of 12 squares (25×25 pixels), as ROI, at the intersection of semicircle and lines (Figure 1). The number of squares for the anterior fixtures was nine. The gray values in these areas were calculated and placed in following formula to obtain the CNR values. (17)

$$CNR = \frac{|Mean_{implant} - Mean_{control}|}{\sqrt{SD_{implant}^2 + SD_{control}^2}}$$

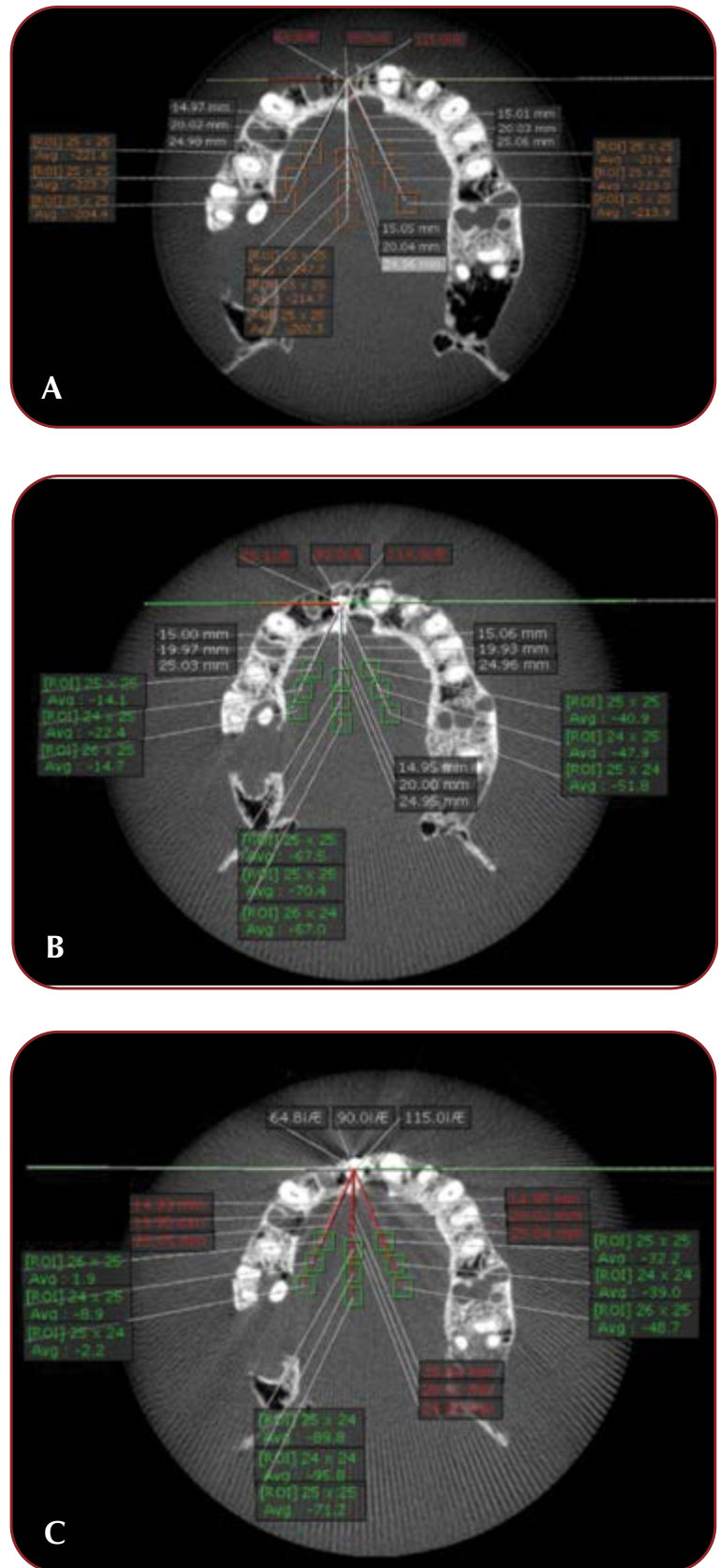


FIGURE 1. CNR calculation method in the maxillary anterior region for control group (A), Roxolid (B), and Zirconium (C).

		Fixture	Number	Mean± SD*	P-Value
Unit	X MIND:	Roxolid	252	1.24± 0.99	0.001
		Zirconium	252	1.17±0.96	
	5G	Roxolid	252	2.74±2.97	0.001
		Zirconium	252	3.28±4.15	
Jaw	Max	Roxolid	252	3.17±2.67	0.001
	Man		252	0.81±1.02	
	Max	Zirconium	252	3.66±3.94	0.001
	Man		252	0.79±0.83	
Site	Anterior (3.3 mm)	Roxolid	216	2.01±2.23	0.21
	Posterior (4.1 mm)		288	1.97±2.42	
	Anterior (3.3 mm)	Zirconium	216	2.66±3.78	0.29
	Posterior (4.1 mm)		288	1.89±2.62	

TABLE 1. Measures of central dispersion of CNR values for Roxolid and Zirconium fixtures by unit, jaw, and region (fixture diameter)

\*SD: standard deviation

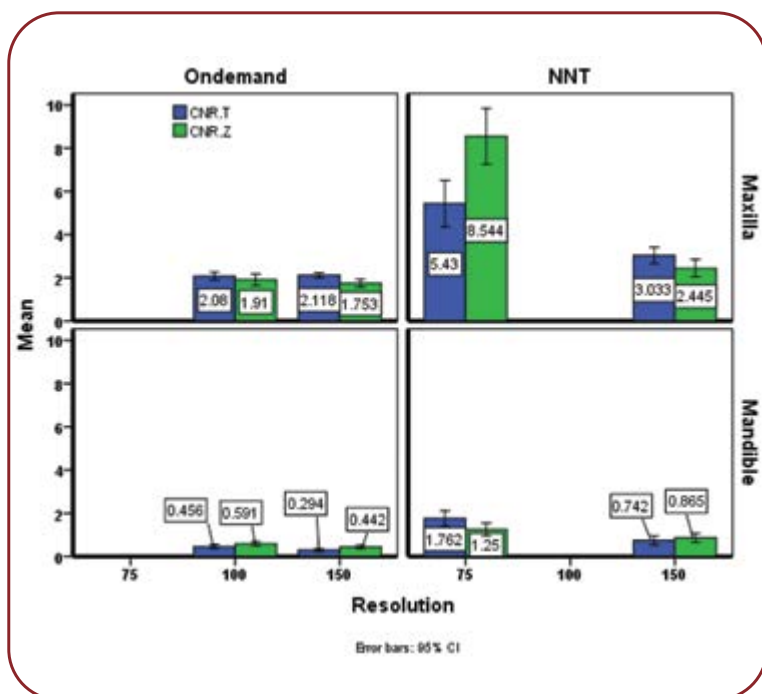


FIGURE 2. Mean CNR values of CBCT images by X MIND and 5G, maxilla and mandible, two resolutions in Roxolid and Zirconium fixtures

The mean, standard deviation, and standard error of CNR values of CBCT images were calculated and reported by fixture material (Roxolid-Zirconium), jaw (mandible-maxilla) resolution

(high-standard), size (anterior-posterior) and section of the images (cervical-middle-apical). The statistical comparison of CNR values by dual-mode variables (fixture material, lower or upper jaw, posterior or anterior, resolution) was done using the paired t-test. In addition, the statistical comparison of CNR values by the triple-mode variable (cervical, middle, apical) was done using the one-way ANOVA (one-sided analysis of variance). □

RESULTS

In contrast to 5G, the mean CNR values of Roxolid fixture in XMIND was higher than Zirconium fixture. Moreover, the CNR values in Roxolid and zirconium fixtures were significantly higher in the maxillary region than the mandibular region (Table 1, Figure 2).

Nevertheless, there was no significant difference between the fixture diameters in terms of the CNR values (Table 1).

Moreover, there was no significant difference between the longitudinal sections of Roxolid and 5G fixtures (cervical, middle, and apical) in terms of CNR values (Table 2).

In XMIND, there was not any significant difference between standard(voxel size: 150 μ) and high (voxel size: 100 μ) resolutions of CBCT images of Roxolid and Zirconium fixtures in term of the CNR values; whereas, in 5G, the CNR value

Unit	Fixture	Number	Resolution (voxel size)*	Mean± SD*	P-Value
X MIND	Roxolid	126	100	1.27±1.01	0.62
		126	150	1.21±0.98	
	Zirconium	126	100	1.25±1.05	0.21
		126	150	1.09±0.87	
5G	Roxolid	126	75	3.59±3.67	0.001
		126	150	1.89±1.67	
	Zirconium	126	75	4.89±5.21	0.001
		126	150	1.65±1.49	

TABLE 3. Measures of central dispersion of CNR values for Roxolid and Zirconium fixtures by resolution

\*XMIND: high resolution =100 μ, standard resolution=150 μ  
 5G: high resolution =75 μ, standard resolution =150 μ

Fixture	Section	Number	Mean± SD*	P-Value
Roxolid	Cervical	168	2.03± 2.23	0.80
	Middle	168	2.05± 2.55	
	Apical	168	1.89± 2.23	
Zirconium	Cervical	168	2.38± 2.98	0.66
	Middle	168	2.23± 3.45	
	Apical	168	2.07± 3.12	

\*SD: standard deviation

TABLE 2. Measures of central dispersion of CNR values for Roxolid and Zirconium fixtures by cervical, middle and apical sections of fixtures

of CBCT images was significantly higher at high resolution (voxel size: 75 μ) than standard resolution (voxel size: 150 μ) (Table 3, Figure 2). □

DISCUSSION

The gray values in CBCT depend on characteristics of the object, such as diameter, shape, density, and atomic number in particular (6, 18, 19). Since metals have high density and their atomic number is higher than soft tissue and bone compositions (20), they cause X-ray beam hardening artifacts while imaging (9, 10). In this study, XMIND and 5G produced different CNR values for the Roxolid and Zirconium fixtures. In XMIND, the CNR of Roxolid fixture was significantly higher than that of Zirconium (1.24 versus 1.17) whereas, in 5G, the CNR of Roxolid

fixture was significantly lower than that of Zirconium (2.74 versus 3.28). According to the inconsistency of different CBCT results given the severity of artifacts caused by titanium and Zirconium, it can be concluded that in addition to the fixture material, the exposure parameters and CBCT Units are also influential (16, 17, 21, 22).

Based on different results reported by Sancho-Puchades’s study into titanium and zirconium fixtures placed in gypsum casts (21), it seems that the difference in anatomic structures, density, and atomic number of tissues adjacent to the fixture site can affect the severity of fixture-related artifacts. Moreover, the CNR values of Zirconium and Roxolid fixtures in the maxilla was significantly higher than those in the mandible, indicating lower incidence of artifacts in the maxilla which is consistent with Machado’s study (16). This difference can be attributed to the difference in the density and thickness of maxillary and mandibular bones.

In this study, the CNR values of different fixture sections (cervical, middle, and apical) were not different, which is inconsistent with Machado’s study. It can be attributed to the presence of crown on the fixtures under examination in Machado’s study, in which the incidence of artifacts was higher in cervical sections (16). □

CONCLUSION

It seems that in addition to the fixture materials, different exposure parameters and CBCT units play a role in the severity of artifacts caused by different fixture alloys. However, such factors as

bone density can affect the severity of artifact, regardless of the fixture alloy. □

*Acknowledgements: We wish to thank all staff of the Department of Oral and Maxillofacial Radiology in Dental School, Babol University of*

*Medical Sciences, for their valuable assistance in this study. This Project was supported by Research Deputy of Babol University of Medical Sciences.*

*Conflicts of interest: none declared.*

*Financial statement: none declared.*

## REFERENCES

1. **Özalp Ö, Tezerişener HA, Kocabalkan B, et al.** Comparing the precision of panoramic radiography and cone-beam computed tomography in avoiding anatomical structures critical to dental implant surgery: A retrospective study. *Imaging Sci Dent* 2018;4:269-275. <https://www.ncbi.nlm.nih.gov/pmc/articles/PMC6305775/>.
2. **Bornstein MM, Scarfe WC, Vaughn VM, Jacobs R.** Cone beam computed tomography in implant dentistry: a systematic review focusing on guidelines, indications, and radiation dose risks. *Int J Oral Maxillofac Implants* 2014;29 Suppl:55-77. <https://www.ncbi.nlm.nih.gov/pubmed/24660190>.
3. **Garib DG, Calil LR, Leal CR, Janson G.** Is there a consensus for CBCT use in Orthodontics? *Dental Press J Orthod* 2014;5:136-149. <https://www.ncbi.nlm.nih.gov/pubmed/25715727>.
4. **Ahmad M, Jenny J, Downie M.** Application of cone beam computed tomography in oral and maxillofacial surgery. *Aust Dent J* 2012;57 Suppl 1:82-94. <https://www.ncbi.nlm.nih.gov/pubmed/22376100>.
5. **Chindasombatjareon J, Kakimoto N, Murakami S, et al.** Quantitative analysis of metallic artifacts caused by dental metals: comparison of cone-beam and multi-detector row CT scanners. *Oral Radiol* 2011;27:114-120. <https://link.springer.com/article/10.1007/s11282-011-0071-z>.
6. **Schulze RK, Berndt D, d'Hoedt B.** On cone-beam computed tomography artifacts induced by titanium implants. *Clin Oral Implants Res* 2010;1:100-107. <https://www.ncbi.nlm.nih.gov/pubmed/19845706>.
7. **Panjnoush M, Kheirandish Y, Mohseni Kashani P, et al.** Effect of exposure parameters on metal artifacts in cone beam computed tomography. *J Dent (Tehran)* 2016;3:143-150. <https://www.ncbi.nlm.nih.gov/pubmed/28392810>.
8. **Jaju PP, Jain M, Singh A, Gupta A.** Artefacts in cone beam CT. *Open J Stomatol* 2013;5:292-297.
9. **Moudi E, Haghanifar S, Madani Z, Bijani A, Nabavi Z.** The effect of metal artifacts on the identification of vertical root fractures using different fields of view in cone-beam computed tomography. *Imaging Sci Dent* 2015;3:147-151. <https://www.ncbi.nlm.nih.gov/pmc/articles/PMC4574051/>.
10. **Yamani Y.** A comparative analysis of different fields of view in cone beam computed tomography imaging to identify the inferior alveolar nerve canal. Master Thesis, 2011, University of Connecticut. <https://www.researchgate.net/publication/265409658>.
11. **Gong XY, Meyer E, Yu XJ, et al.** Clinical evaluation of the normalized metal artefact reduction algorithm caused by dental fillings in CT. *Dentomaxillofac Radiol* 2013;4:20120105. <https://www.ncbi.nlm.nih.gov/pmc/articles/PMC3667513/>.
12. **Ibraheem I.** Reduction of artifacts in dental cone beam CT images to improve the three dimensional image reconstruction. *J Biomed Sci Eng* 2012;8:409-415. <https://www.scirp.org/journal/PaperInformation.aspx?PaperID=21455>.
13. **Barrett JF, Keat N.** Artifacts in CT: recognition and avoidance. *Radiographics* 2004;Nov-Dec;24(6):1679-1691. <https://pubs.rsna.org/doi/10.1148/rg.246045065>
14. **Makins SR.** Artifacts interfering with interpretation of cone beam computed tomography images. *Dent Clin N Am* 2014;58:485-495. <https://www.ncbi.nlm.nih.gov/pubmed/24993920>.
15. **Abramovitch K, Rice DD.** Basic principles of cone beam computed tomography. *Dent Clin N Am* 2014;58:463-484. <https://www.ncbi.nlm.nih.gov/pubmed/24993919>.
16. **Machado AH, Fardim KAC, de Souza CF, et al.** Effect of anatomical region on the formation of metal artefacts produced by dental implants in cone beam computed tomographic images. *Dentomaxillofac Radiol* 2018;3:20170281. <https://www.ncbi.nlm.nih.gov/pubmed/29231055>.
17. **Fontenele RC, Nascimento EH, Vasconcelos TV, et al.** Magnitude of cone beam computed tomography image artifacts related to zirconium and titanium implants: impact on image quality. *Dentomaxillofac Radiol* 2018;18:20180021.
18. **Oliveira ML, Tosoni GM, Lindsey DH, et al.** Influence of anatomical location on CT numbers in cone beam computed tomography. *Oral Surg Oral Med Oral Pathol Oral Radiol* 2013;115:558-564. <https://www.ncbi.nlm.nih.gov/pubmed/29668300>
19. **Langland O, Langlais R, Preece J.** The X ray machine, attenuation and recording of radiographic images. *Principles of Dental Images*. 2<sup>nd</sup> ed, Philadelphia: Lippincott William & Wilkins, 2002, pp 31-51.
20. **Cremonini CC, Dumas M, Pannuti CM, et al.** Assessment of linear measurements of bone for implant sites in the presence of metallic artefacts using cone beam computed tomography and multislice computed tomography. *Int J Oral Maxillofac Surg* 2011;8:845-850. <https://www.ncbi.nlm.nih.gov/pubmed/21621979>.
21. **Sancho-Puchades M, Hämmerle CH, Benic GI.** In vitro assessment of artifacts induced by titanium, titanium-zirconium and zirconium dioxide implants in cone-beam computed tomography. *Clin Oral Implants Res* 2015;10:1222-1228. <https://www.ncbi.nlm.nih.gov/pubmed/25040484>.
22. **Smeets R, Schöllchen M, Gauer T, et al.** Artefacts in multimodal imaging of titanium, zirconium and binary titanium-zirconium alloy dental implants: an in vitro study. *Dental Maxillofac Radiol* 2017;2:20160267. <https://www.ncbi.nlm.nih.gov/pubmed/27910719>.